



Cite this: *RSC Adv.*, 2024, **14**, 28260

Selecting appropriate cellulose morphology to enhance the nitrogen content of nitrocellulose†

Raden Reza Rizkiansyah, ^a Y. Mardiyati, ^{*a} Arief Hariyanto^b and Tatacipta Dirgantara^c

This study aims to determine the effect of cellulose morphology on enhancing the nitration of cellulose to achieve nitrocellulose with a high nitrogen content. Cotton linter was employed as a point of reference, and *Luffa cylindrica* and coffee pulp cellulose were used for comparison. *Luffa cylindrica* and coffee pulp cellulose were used considering their distinctive morphological characteristics compared to cotton linter. They were nitrated at room temperature for 60 minutes using a mixture of technical grade nitric acid and sulfuric acid with a nitric acid:sulfuric acid ratio of 1:3 and cellulose:nitric acid ratio of 1:45. The results showed that luffa cellulose is similar in characteristics to cotton linter, which exhibits short, thin-walled tubular ribbon-like microfibrils with 75.09% crystallinity and a specific surface area of 0.70 $\text{m}^2 \text{ g}^{-1}$. Nitration of luffa cellulose resulted in nitrocellulose with a nitrogen content as high as 13.67%, which is higher than that of cotton linter with a value of 13.49%. This value of nitrogen content was high enough to be applied even in military-grade applications. Morphology was revealed as the most influential characteristic of nitration, which allows for the preparation of nitrocellulose with qualities similar to cotton linter-based nitrocellulose. Thus, it was demonstrated that nitrocellulose with a high nitrogen content could be achieved despite using a technical grade nitration reagent by selecting cellulose with an appropriate morphology.

Received 7th June 2024
 Accepted 15th August 2024

DOI: 10.1039/d4ra04172k
rsc.li/rsc-advances

Introduction

Nitrocellulose (NC) is the earliest derivative product of cellulose discovered and is historically known as the first semi-synthetic plastic produced. Currently, NC applications in the plastic industry are mostly replaced by synthetic polymers. However, nitrocellulose is still applied in some specialized applications, such as biofilter materials,¹ support for protein immobilization,² coating,³ and military application.⁴

The utilization of NC in modern times is mostly related to military applications, such as propellants for firearm ammunition or rocketry.⁵ The possibility of applying NC for this purpose was first emphasized by Schonbein in 1845, who suggested that it could be an alternative to firearm gunpowder, and thus, it was termed as guncotton.⁵ This capability stems from the energetic nature of NC, which is credited to the presence of

the nitrate group (ONO_2) in its molecular structure. Overall, the molecular structure of NC provides both oxidizing and reducing groups for combustion reactions, allowing it to diminish the need for atmospheric oxygen.^{4–7} The decomposition of NC also releases a high amount of energy as an exothermic reaction due to the formation of nitrogen (N_2) as combustion products.^{8,9} These characteristics allow NC to comply with the required energetic properties for propellant and low-explosive applications.

The application of NC is determined by its nitrogen content, which results from the substitution of the hydroxyl group on cellulose to the nitrate group through the nitration process, as illustrated in Fig. 1. The nitrogen content of NC determines its physical and mechanical properties, solubility, and energetic properties.^{6,10} This is because the hydroxyl group is responsible for the inter- and intra-crystalline bonding in cellulose. Substituting hydroxyl groups with other groups would disrupt these bonds, thus changing the properties of cellulose.⁶ NC, with a nitrogen content of around 11.5–12.2%, is usually used for civil applications, such as plastics and coating. On the other hand, military propellants require a higher nitrogen content that is greater than 13%, as they need a higher energy output.^{4,11,12}

NC is commonly manufactured from cotton linter (CL), especially for military propellant application. The manufacture of NC involves the usage of a mixture of nitric acid and

^aMaterial Science and Engineering Research Group, Faculty of Mechanical and Aerospace Engineering, Institut Teknologi Bandung, Jl. Ganesh 10, Bandung 40132, Indonesia. E-mail: mardiyati@material.itb.ac.id

^bFluid Dynamics and Propulsion Research Group, Faculty of Mechanical and Aerospace Engineering, Institut Teknologi Bandung, Jl. Ganesh 10, Bandung 40132, Indonesia

^cSolid Mechanics and Lightweight Structures Research Group, Faculty of Mechanical and Aerospace Engineering, Institut Teknologi Bandung, Jl. Ganesh 10, Bandung 40132, Indonesia

† Electronic supplementary information (ESI) available. See DOI: <https://doi.org/10.1039/d4ra04172k>



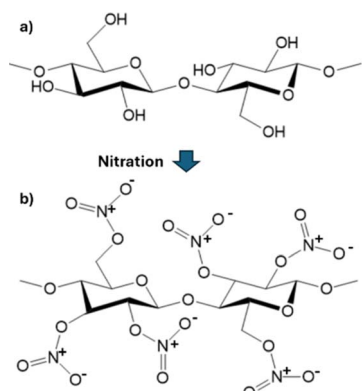


Fig. 1 Change in the cellulose structure as a result of substitution through the nitration process: (a) cellulose and (b) nitrocellulose (NC).

sulfuric acid as the nitration reagent.⁴ Despite its long-standing use as the major source of NC and cellulose derivatives in general, the utilization of cotton linter raises concerns about environmental impacts, such as high freshwater and terrestrial ecotoxicity by pesticides, as an effect of its production method.¹³ Attempts to utilize alternative cellulose sources from other plants or agricultural wastes for NC have been researched as an approach to solving this problem. The limitation of cotton linter provisions in regions where cotton was difficult to grow became another matter that served as a driving factor in these developments. Several previously reported biomass sources have been evaluated as sources of cellulose for nitrocellulose, such as empty palm oil bunch,¹⁴ miscanthus,¹⁵ peanut husks,¹⁶ pineapple leaves,¹⁷ alfa grass,¹⁸ bamboo,¹⁹ *Acacia mangium*,²⁰ brown algae,¹⁰ sansevieria,²¹ and bacterial cellulose.⁶ However, these biomass sources still yielded nitrocellulose with a nitrogen content of under 13%, thus making them unsuitable for applications that require a high nitrogen content (such as military propellant), limiting its usage. Utilization of fuming nitric acid was another approach that was reported to be capable of yielding nitrocellulose with a high nitrogen content.²²⁻²⁴ However, its usage on an industrial scale would be difficult due to its hazardous and corrosive nature.

The inherent chemical reactivity and steric hindrance stemming from the nitration reagent or cellulose supramolecular structure are factors that determine the reactivity of cellulose.²⁵ This condition prompts the consideration of the accessibility of the hydroxyl group of cellulose since it potentially affects the ease of the nitration reaction, especially in achieving NC with a high nitrogen content. Crystallinity and morphological features are characteristics that could affect the accessibility in cellulose.²⁵⁻²⁷ This characteristic could differ depending on the source of cellulose and preliminary treatment.¹⁰ It was also reported that the choice of cellulose source could affect the NC's physicochemical and energetic features.¹⁰ Despite their importance, the significance of these characteristics on the nitration process was rarely discussed or considered in previous reports that attempted to develop alternative cellulose sources.

In this study, cellulose from *Luffa cylindrica* (LC) and coffee pulp waste (CP) was used to evaluate the significance of cellulosic characteristics to enhance the high nitrogen content from the nitration process, with CL as a point of reference. Both reported sources have different cellulose morphologies and characteristics. LC is a Cucurbitaceae family plant with elongated fruits and net-like fibrous vascular system endocarp, continuous hollow struts, and porous microcellular architecture.²⁸ Its fibers are categorized as seed fibers, along with cotton and kapok fibers.²⁹ The cellulose of LC was reported to have a distinctive morphology, as it could have spiral-shaped,³⁰ network-like, and fibrillar microfibrils.³¹ These characteristics could be beneficial to the nitration process, providing a more accessible hydroxyl group. CP is a post-harvesting waste resulting from discarded parts of the coffee cherry. Previous work found that the CP cellulose showed helical-shaped microfibrils embedded between the dense, smooth surfaces, possibly formed by packing numerous smaller fibers.³² This condition results in cellulose with limited accessibility compared to LC cellulose, thus providing contrasting properties to the latter. To further evaluate these properties, CL, the common source of NC, would be used as a point of reference for both types of cellulose. The basic characteristics of cellulose would be evaluated in terms of their morphology, specific surface area, and crystallinity using scanning electron microscopy (SEM), Brunauer-Emmett-Teller (BET), and X-ray diffraction (XRD), respectively. All cellulose materials were nitrated under the same condition before being characterized in terms of their nitrogen content and change of crystalline parameters. This study is expected to show the relationship between the cellulose characteristics and the effectiveness of the nitration process, especially in the nitrogen content of the resulting NC. Therefore, through this work, determining the appropriate cellulose morphology could be a viable strategy to achieve nitrocellulose with high nitrogen content, and simultaneously develop a more sustainable alternative source of cellulose for nitrocellulose apart from cotton linter.

Experimental

Materials

Arnold Grummer's cotton linter was purchased from National Arts Supply, USA, which was used as a point of reference. Cotton linter was used without any further chemical treatment and was only subjected to oven drying at 60 °C to constant weight before use. *Luffa cylindrica* (LC) was provided by *Omah Loofah* from a plantation in the Denanyar district, Jombang regency, Indonesia. Furthermore, arabica coffee (*Coffea arabica*) pulp waste (CP) was procured from *Kawung Asli*, based from the Cikajang coffee plantation, Garut Regency, Indonesia. Both LC and CP were obtained in sun-dried conditions, and dried at 60 °C to a constant weight before use. Sodium hydroxide (NaOH) and hydrogen peroxide (H₂O₂) were procured from Glatt Chemical, Inc. Sodium hypochlorite (NaClO) solution (12 wt%) was supplied from Bixxon Chemical, Inc. Analytical grade SMART LAB sulfuric acid with a purity of 97 wt% was bought from Quimica Jaya Perkasa, Inc. The technical grade nitric acid



(65 wt%) and sulfuric acid (98 wt%) used for the nitration reagent mixture were purchased from Rofa Laboratory, Inc. and Glatt Chemical, Inc., respectively.

Cellulose isolation from *Luffa cylindrica*

Sequential sodium hydroxide alkali treatment and bleaching using sodium hypochlorite were conducted to isolate cellulose from *Luffa cylindrica*. LC was cut into 4 cm pieces before treatment. A 4 wt% sodium hydroxide solution was employed for the alkali treatment process of LC. The process was conducted at 80 °C for 2 hours. This process resulted in alkali-treated luffa cuts (ATL), which were filtered, washed, and dried under ambient temperature before further processing.

The second stage of cellulose isolation from LC involves bleaching dried ATL using a 5.3 wt% sodium hypochlorite solution for 15 minutes at 80 °C. The result was also filtered, washed, and dried at room temperature. This stage resulted in *Luffa cylindrica* cellulose (LCC). The dried, agglomerated LCC was ground and sieved using a 60 mesh sieve before the subsequent processing.

Cellulose isolation from *Coffea arabica* pulp waste

Isolation of cellulose from arabica coffee pulp waste involved sodium hydroxide alkali treatment and hydrogen peroxide bleaching.³² The dried CP was first dried using an oven at 60 °C for one hour before milling and sifting using a 2 mm opening sieve. Sieved CP (SCP) was obtained from this process. Furthermore, it was stirred in demineralized water at 60 °C for 120 minutes to remove its water-soluble substances, resulting in washed CP (WCP). Alkali treatment was conducted on the dried WCP using 3 wt% sodium hydroxide solution at 80 °C for 2 hours. The obtained alkali-treated CP slurry (wet condition) was washed to neutral pH, and then sieved using a 40 mesh sieve to separate residual coffee beans. The obtained filtrate was then dried under ambient temperature, resulting in alkali-treated CP (AT-CP).

The residual non-cellulosic content on AT-CP was removed using hydrogen peroxide bleaching. Bleaching was conducted to AT-CP using 10 wt% hydrogen peroxide solution at a temperature of 80 °C for 2 hours. The bleached AT-CP was filtered, washed, and dried at room temperature. The resulting product from this stage was designated as CP cellulose (CPC).

Preparation of nitrocellulose

Preparation of NC involves the use of a nitric acid–sulfuric acid mixture as the nitration reagent. The used nitric acid and sulfuric acid reagents were technical grade with concentrations of 65 wt% and 98 wt%, respectively. The nitration process was conducted at room temperature for a nitration duration of 60 minutes by dispersing CL, LCC, or CPC in the nitration solution with a fixed nitric acid:sulfuric acid ratio of 1:3 (v/v) and cellulose:nitric acid ratio of 1:45 (w/v). The nitration was followed by filtering and washing the nitrated product to a neutral pH. Furthermore, the nitration products were stirred in boiling demineralized water for 15 minutes before being filtered. The results were designated as CL-NC, LC-NC, and CP-NC for the CL,

LCC, and CPC-based nitrocellulose, respectively. NCs were kept in water-wet condition. The sample were air-dried and kept in a desiccant beads-filled desiccator to constant weight prior to characterization/testing.

Characterization and testing

The lignocellulosic content of CL, LCC, and CPC were evaluated using Chesson's method,³³ which employs four stages. The first stage involves stirring 1 gram (a) of dried sample in 150 ml boiling water for 2 hours. The result was then filtered and dried to constant weight (b). The first-stage residue was then refluxed in 150 ml of boiled 0.5 M sulfuric acid (H_2SO_4) for 2 hours. The residue was then filtered, washed to neutral pH, and dried to constant weight (c). The final stage of Chesson's method involves dispersing and stirring the second-stage dried residue in 10 ml of 72 wt% sulfuric acid for 4 hours. Water was then added to the mixture to dilute it to obtain a 0.5 M solution concentration of sulfuric acid and stirred for 2 hours at 100 °C. The residue was then filtered and dried to constant weight (d). Respective water soluble content, hemicellulose, cellulose, and lignin content percentage values were calculated using equations in Table 1.

The CL, LCC, and CPC morphology were evaluated using Scanning Electron Microscopy (SEM). SEM characterizations were conducted using the JEOL JSM 6510 (JEOL Ltd., Tokyo, Japan) with an applied voltage of 10 kV.

Crystallinity and lattice properties were evaluated through X-ray diffraction (XRD) characterization. XRD was conducted using a Rigaku MiniFlex X-ray Diffractometer, which records diffraction spectra at 2θ in the range of 10°–90°.

The BET method was used to characterize the specific surface areas of CL, LCC, and CPC. The Quantachrome Nova 4200e BET Surface Area and Pore Size Analyzer were utilized for this purpose.

A Thermo Scientific Elemental Analyzer was used to evaluate the nitrogen content of the resulting nitrocellulose prepared from CL, LCC, and CPC.

Fourier Transform Infrared (FTIR) spectroscopy characterization was conducted to evaluate the presence of the nitrate group after the nitration process was determined from the resulting FTIR spectra. The sample was prepared as a pellet with

Table 1 Equations used for lignocellulosic content calculation using Chesson's method^a

Content	Calculation
Water soluble content (%)	$\frac{a - b}{a} \times 100\%$
Hemicellulose	$\frac{b - c}{a} \times 100\%$
Cellulose	$\frac{c - d}{a} \times 100\%$
Lignin	$\frac{d}{a} \times 100\%$

^a a: initial weight. b: dried residue of stage 1 (after boiling in water). c: dried residue of stage 2 (after refluxed in 0.5 M sulfuric acid). d: dried residue of final stage.



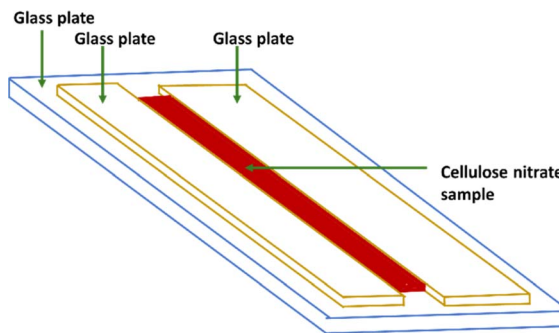


Fig. 2 Illustration of sample placement for burning rate testing.

KBr. A Prestige 21 Shimadzu (Japan) was used for the characterization with the spectra recorded in the 4000 cm^{-1} to 500 cm^{-1} range.

Burning tests were applied to NC prepared from CL, LCC, and CPC. This test was conducted as a quantitative evaluation of the NC through its flame characteristics, and to measure the burning duration and rate of each NC. Around 0.25 g of NC sample was used for the burning test, which was placed on a glass plate. The burning was triggered using an electric arc igniter. The burning rate was evaluated by burning 0.15 g of NC set in an elongated fashion, as illustrated in Fig. 2. Works reported by Liu (2018) and Zhang (2014) were used as a reference for this testing.^{34,35} The Sony Alpha 7 IV camera recorded the burning process at a 120 fps frame rate. The recordings were used to evaluate the burning characteristics and measure the burning rate.

Results and discussion

Characteristic of cotton linter, *Luffa cylindrica*, and *Coffea arabica* pulp celluloses

LC and CP underwent the respective alkali treatment and bleaching process.^{32,36} Alkali treatment was conducted to remove the non-cellulosic content from the respective lignocellulosic biomass. The bleaching process was used to remove the residual non-cellulosic content, especially lignin, which contributes to the brownish color of the lignocellulosic biomass that is still left after alkali treatment.^{37,38} These isolation processes resulted in *Luffa cylindrica* cellulose (LCC) and coffee pulp cellulose (CPC), respectively.

The visual appearance of CL, LC, and CP are presented in Fig. 3. Native, alkali-treated, and cellulose isolated were also included for comparison. The result showed that both LC and CP changed in appearance, color, and form after alkali treatment and bleaching. After alkali treatment, AT-LC still had similar conditions and a slightly faded color compared to its original native form, and AT-CP changed into a paper-like appearance with a brownish color. These conditions indicate a significant amount of non-cellulosic content that is still present, thus allowing a similar appearance to the original form (in terms of form for AT-LC and color for AT-CP). Significant changes were shown in post-bleaching condition, where LCC and CPC changed into brighter colors. LCC is also shown to be

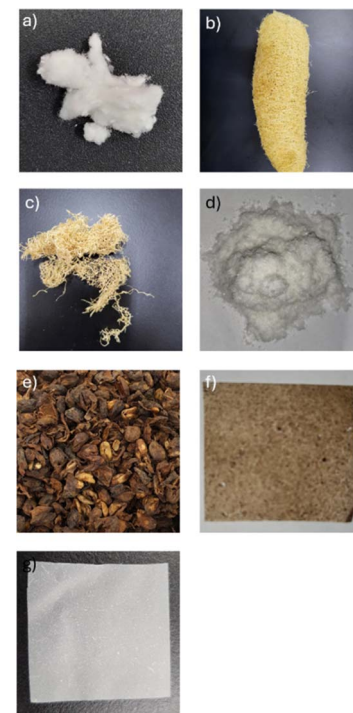


Fig. 3 Visual appearance: (a) cotton linter (CL), (b) native *Luffa cylindrica* (LC), (c) alkali-treated *Luffa cylindrica* (AT-LC), (d) *Luffa cylindrica* cellulose (LCC), (e) coffee pulp waste (CP), (f) alkali-treated coffee pulp waste (AT-CP), and (g) coffee pulp waste cellulose (CPC).

reduced into smaller particles. This change into a bright color indicates the removal of lignin.³⁹ The reduction of the fiber into smaller particles is caused by the removal of non-cellulosic content (lignin and hemicellulose), which keeps the fiber structure intact. Thus, the absence of these components leads to the disintegration of fiber and release of individual cellulose fibrils.^{40,41}

Fig. 4 presents the lignocellulosic content of CL, native LC, and CP, and their post-bleaching products (LCC and CPC) based on the result of Chesson's method. The result confirms the removal of non-cellulosic content, as demonstrated by the

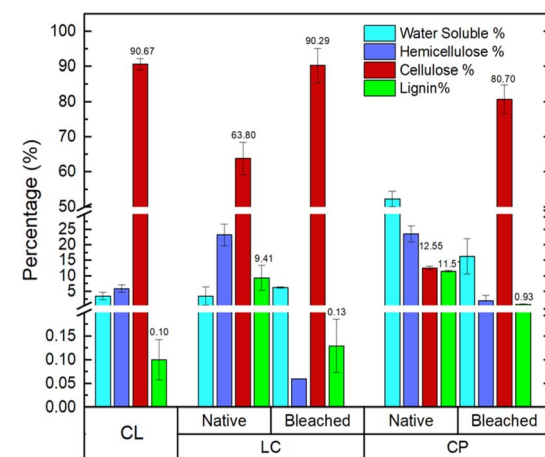


Fig. 4 Lignocellulosic content of CL compared to native and bleached LC and CP.

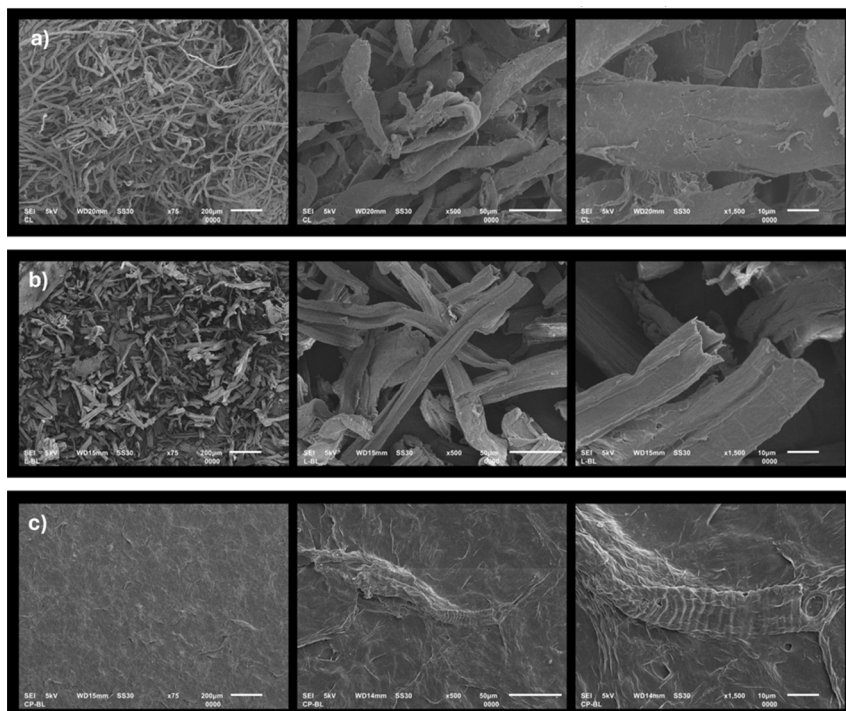


Fig. 5 SEM image of cellulose: (a) CL, (b) LCC, and (c) CPC.

visual appearance. CL comprises 90.67% cellulose, while LCC and CPC have 90.29% and 80.70%, respectively. LCC was most similar in terms of cellulose fraction to CL. However, all of the cellulose obtained had a cellulose fraction of at least more than 80%.

The morphological characteristics of CL, LCC, and CPC were evaluated using SEM. SEM photomicrographs of each sample are shown in Fig. 5. The result showed that each cellulose has distinctive morphological features. CL features a curly, cylindrical fiber with a smooth, non-porous surface with a diameter of around $\pm 28.67 \mu\text{m}$. LCC was shown to have a short, thin-walled tubular ribbon-like microfibril morphology, with length and diameter of around $254.82 \pm 50.43 \mu\text{m}$ and $\pm 23.52 \mu\text{m}$, respectively. CPC possessed a flat and dense surface appearance, with some spiral-shaped fibrils embedded between. Morphologically, LCC is the most comparable to the CL. LCC and CL present a cylindrical fibrous morphology with similar diameters despite having shorter fibers than CL, which could extend as long as 2000–6000 μm in length.^{42,43}

XRD characterizations were conducted to evaluate the crystallinity of CL, LCC, and CPC. Diffraction spectra of CL, LCC, and CPC are shown in Fig. 6. The spectra presenting diffraction peaks at 15° , 16.5° , and 22.5° suggest a typical crystallinity pattern of cellulose I polymorph of natural cellulose.⁴⁴ The crystallinity of each cellulose was calculated from the obtained diffraction spectra using eqn (1).

$$\text{IC} = \frac{I_{002} - I_{\text{am}}}{I_{002}} \times 100\% \quad (1)$$

where IC is the crystallinity, while I_{002} and I_{am} are intensity values of crystalline and amorphous phases, respectively.⁴⁵

Fig. 7 presents the calculated crystallinity results of CL, LCC, and CPC. This shows that CL has comparable crystallinity to LCC, while CPC has a lower crystallinity than the latter.

Cellulose is a polycrystalline material, which consists of a portion of an orderly arranged cellulosic chain (crystalline region) and another portion of a more disordered part (amorphous region).^{7,46} Crystallinity is a measure of the regularity of the cellulose arrangement. High crystallinity reflects the cellulose possessing a high portion of an orderly arranged cellulosic chain.^{46,47} CL and LCC have a crystallinity of about 75%. This was higher than CPC, which possesses a crystallinity of approximately 59%. The result indicates that after nitration, a higher nitrogen content could be achieved in CL and LCC than in CPC. The estimate is based on some previous studies, which

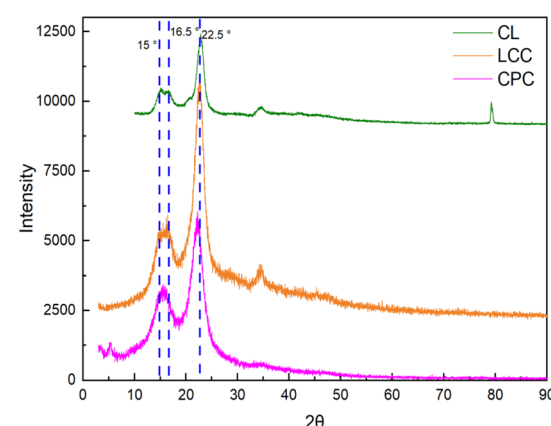


Fig. 6 X-ray diffractogram of CL, LCC, and CPC.



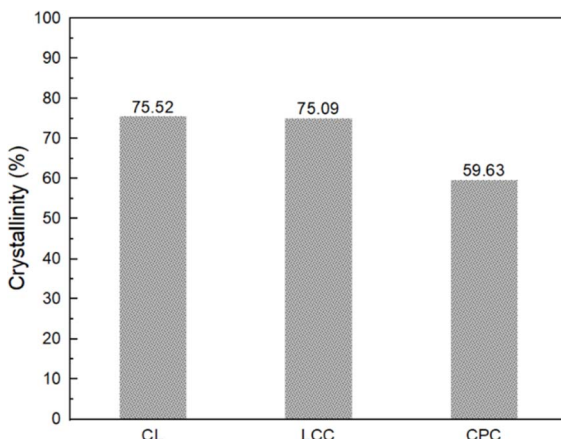


Fig. 7 Crystallinity of CL, LCC, and CPC calculated from the XRD diffractogram.

reported that cases of higher nitrogen content could be obtained by the use of cellulose with higher crystallinity.^{18,48} This was caused by the higher portion of the α -cellulose present in higher crystallinity, which allows a higher yield of the derivative product and improved diffusion of the nitronium ion.^{18,48}

BET characterization was conducted to evaluate the specific surface area of CL, LCC, and CPC. Specific surface areas resulting from BET characterization for LC, LCC, and CPC are shown in Fig. 8. The result showed that LCC and CPC had a higher specific surface area than CL. Cellulose with a higher specific surface area supposedly has a more readily accessible hydroxyl group, which is more advantageous for nitration reactions.^{49–51} However, better substitution does not always guarantee a higher specific surface area as an effect of the non-specific preference of cellulose absorption.²⁰

Relationship of cellulose characteristics and effectiveness of cellulose nitration

The overall evaluation of cellulose characteristics based on SEM, XRD, and BET results suggests that each cellulose stem

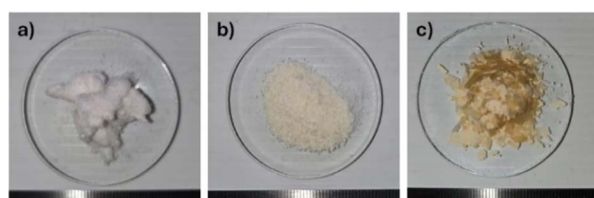


Fig. 9 Visual appearance of nitrocellulose: (a) CL-NC, (b) LC-NC, and (c) CP-NC.

from different sources could have distinct properties. Distinctive morphology, crystallinity, and surface area potentially provide accessibility of the hydroxyl group to nitronium ions, leading to effective nitration. Nitration was conducted for each CL, LCC, and CPC to evaluate this matter. Nitration using a mixture of nitric acid and sulfuric acid with fixed nitric acid : sulfuric acid ratio of 1 : 3 (v/v); cellulose : nitric acid ratio of 1 : 45 (w/v); and nitration duration of 60 minutes at room temperature were conducted to obtain CL-NC, LC-NC, and CP-NC, respectively. Nitric acid serves as a source of nitronium ion (NO_2^+) that would react with the hydroxyl group of cellulose to form the nitrate group.^{4,7,52,53} Sulfuric acid plays a role in the nitration reaction to catalyze the formation of nitronium ion (from nitric acid), dehydration of water molecules, and swelling of cellulose.^{54–56}

The visual appearance of CL-NC, LC-NC, and CP-NC are shown in Fig. 9. The result indicates that LC-NC and CP-NC yielded a yellowish color compared to CL-NC and the original LCC and CPC. This condition is caused by the reaction between sulfuric acid and residual non-cellulosic content in the cellulose.⁵⁷

Elemental analysis was utilized to quantitatively evaluate the nitrogen content of CL-NC, LC-NC, and CP-NC. The analysis showed that CL-NC, LC-NC, and CP-NC resulted in different nitrogen contents despite being nitrated under similar fixed nitration conditions. LCC presents the highest nitrogen content, which reached about 13.67%, followed by the slightly lower CL-NC value of 13.49%. CP-NC resulted in the lowest nitrogen content compared to CL-NC and LC-NC, which was only about 8.05%. The result suggests that cellulose with similar morphology and characteristics could have comparable post-nitration qualities.

FTIR characterizations were conducted on CL, LCC, CPC, CL-NC, LC-NC, and CP-NC to confirm the presence of the nitrate group, which substitutes the hydroxyl group after the nitration process. The resulting FTIR spectra of pre- and post-nitrated products are shown in Fig. 10. The spectra were normalized to the 1160 cm^{-1} peak, which corresponds to the C–O–C glycosidic stretching of cellulose.^{58,59} This peak was used for normalization because the group was unaffected and was not involved in a substitution reaction. The result indicates that compared to its pre-nitrated condition, CL-NC, LC-NC, and CP-NC presented new absorbance peaks at 1660 cm^{-1} (asymmetric stretching of NO_2), 1280 cm^{-1} (symmetric stretching of NO_2), 840 cm^{-1} (O– NO_2 stretching), 765 cm^{-1} (asymmetric deformation of the O– NO_2 group), and 690 cm^{-1} (symmetric deformation of the O– NO_2 group).

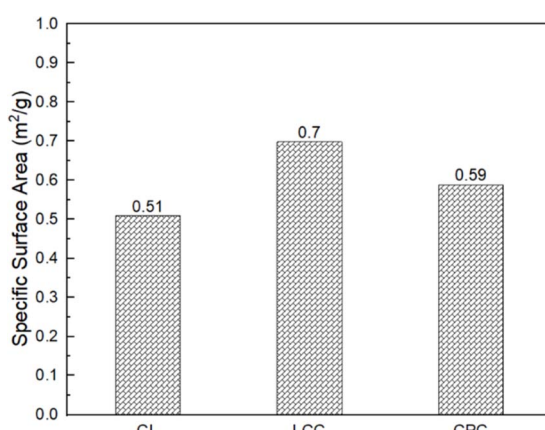


Fig. 8 Specific surface area of cellulose based on BET characterization of CL, LCC, and CPC.



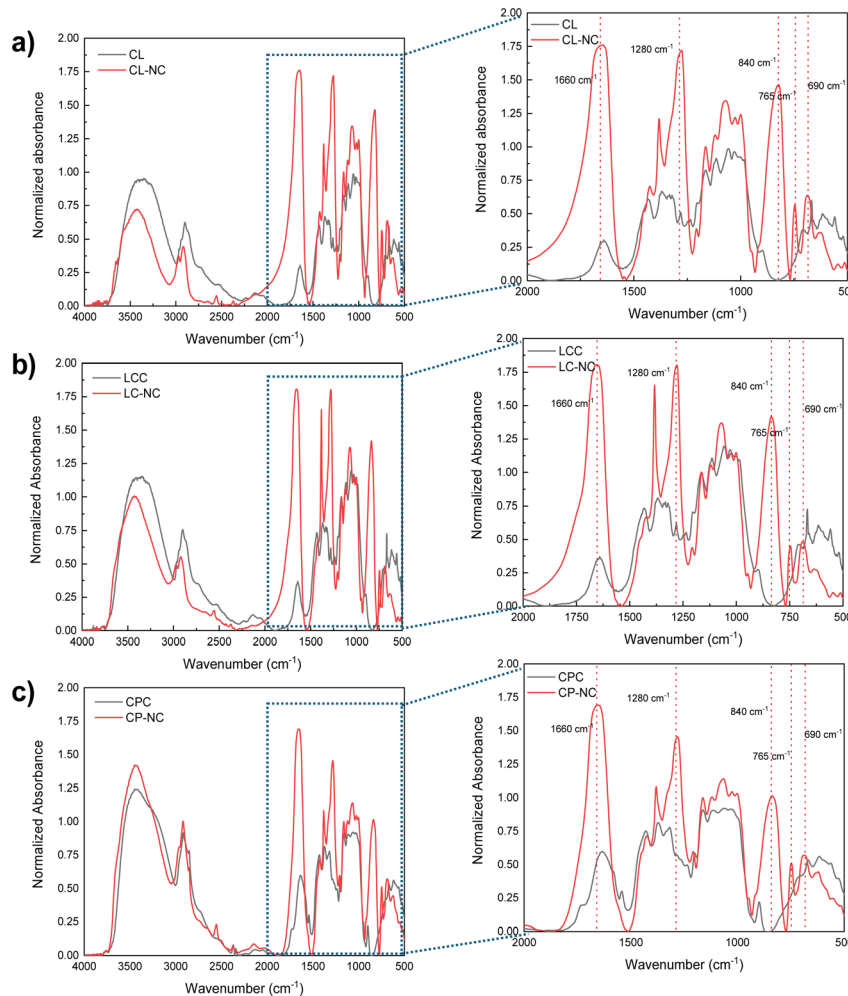


Fig. 10 FTIR spectra of cellulose and nitrocellulose from the respective sources: (a) CL-NC, (b) LC-NC, and (c) CP-NC.

NO_2 group), which indicating the presence of the nitrate group.^{18,60} This result suggests that the hydroxyl groups have been substituted with the nitrate group.

The nitration process could change the crystallographic plane spacing (d_{hkl}) of cellulose. This shift in d_{hkl} is caused by the larger size of the nitrate group that substitutes the hydroxyl group, resulting in an increased distance between the cellulose chain.^{4,5,61,62} The change in the crystallographic plane spacing would increase with the number of substituted hydroxyl groups.⁵ To confirm this phenomenon, XRD characterizations were employed for CL-NC, LC-NC, and CP-NC. A change in the d_{hkl} of the 101 plane was used to indicate the effect of the increase in nitrogen content.^{6,57} The 101 plane was represented by the peak around 2θ in the range of 14° – 16° in diffraction spectra, as highlighted in Fig. 11.^{6,57} The result showed that in CL-NC and LC-NC, its diffraction spectra exhibited a change in pattern and shift of the 101 plane peaks to a lower diffraction angle compared to its pre-nitrated condition. However, in CP-NC, this remains unchanged. This shifting to a lower diffraction angle indicates a change in the crystallographic plane spacing.⁵ The dimensions of the plane spacing were calculated

from the diffraction angle of the 101-peak using Bragg's law (eqn (2)).⁶³

$$d = \frac{n\lambda}{2 \sin \theta} \quad (2)$$

where d , n , λ , θ are the plane spacing dimension, diffraction order, X-ray wavelength, and diffraction angle, respectively. The result showed a difference in dimension spacing between each cellulose, with LCC having the widest, followed by CL and CPC, as shown in Fig. 12. In CL and LCC, the interplanar dimension of post-nitrated cellulose increased compared to its pre-nitrated condition. However, the pre- and post-nitrated interplanar dimensions showed no difference in CPC. The increase of the interplanar dimension in CL and LCC indicates the presence of nitrate groups. In contrast, the unchanged interplanar dimension of CPC suggests a lower amount of nitrate groups, which could suggest that its fiber characteristic is unaccommodating for a higher number of nitrate groups.⁵ LCC is also shown to have a slightly higher interplanar dimension than CL. This suggests that LCC has a higher nitrogen content than CL, which is consistent with its evaluated nitrogen content.



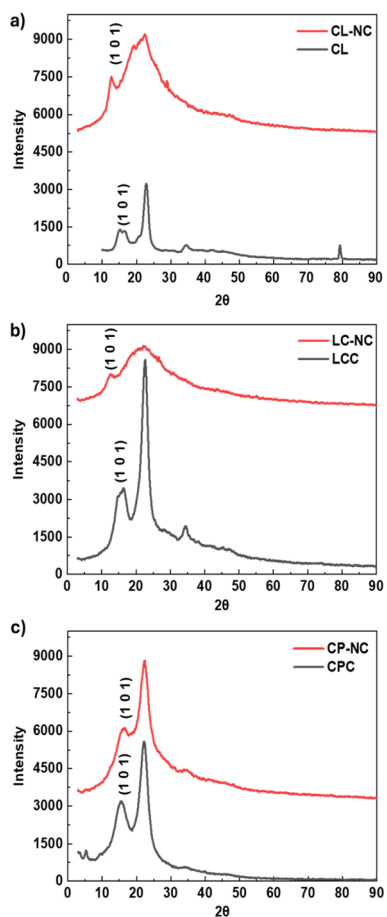


Fig. 11 Diffraction spectra: (a) CL and CL-NC, (b) LCC and LC-NC, (c) CPC and CP-NC.

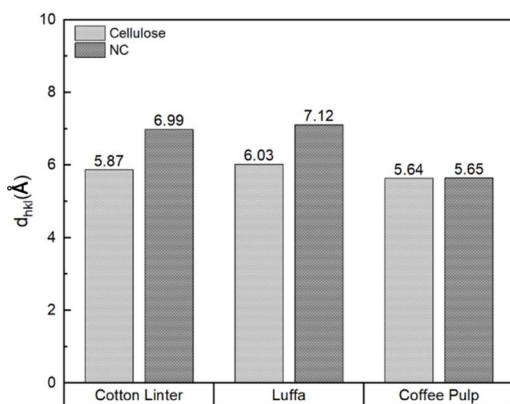


Fig. 12 Interplanar dimension of the 101 plane for CL, LC, and CP in pre- and post-nitration conditions.

Table 2 summarizes the relationship between nitrogen content and the respective cellulose characteristics. The result of this study showed that the usage of cellulose with different characteristics would affect the resulting nitrocellulose. LCC had the highest nitrogen content among the different cellulose

materials used, with a value of 13.67%, which is slightly higher than that of CL at about 13.49%. This degree of nitrogen content was suitable even in military propellant applications, which require a minimum of 13.5% nitrogen content for guncotton-grade NC.⁶⁴ Based on the evaluated characteristic, the morphology could significantly affect the nitration reaction before considering the crystallinity and specific surface area. This conclusion is based on comparing the results to the CPC nitration. Despite having a lower crystallinity than LCC and CL and a higher surface area than CL, CPC has a lower nitrogen content. This could be caused by its morphology, which consists of a dense layer on its surface that potentially hinders the movement of nitronium ions, leaving most of the cellulose unnnitroated. This is also indicated by the XRD characterization of CP-NC, which showed no increase in the 101 crystalline plane spacing dimensions. It confirms that most of the hydroxyl part is unnnitroated and stays in its original form. LCC has similar fibrillar microfibril characteristics to CL, the common source of NC, with a slightly lower crystallinity and higher specific surface area than the latter. Its smaller fiber length possibly contributes to its higher surface area. On the other hand, the morphological condition of CL and LCC could allow for easier access to hydroxyl groups with lower steric hindrance, leading to an increase in nitronium ion diffusion and adsorption to cellulose molecules.¹⁸ This condition contributes to a similar nitrogen content with CL-NC (with LC-NC having slightly higher nitrogen content). This trend is also confirmed by XRD characterization of LC-NC and CL-NC, wherein the former has a larger 101 crystalline plane spacing than the latter, indicating a higher nitrogen content. Thus, these results clearly prove that the morphology of the cellulose could be an affecting factor in the nitration process.

Burning tests were conducted to evaluate the nitrated products qualitatively through their flame characteristics, and to measure their burning duration and burning rate. NC samples were ignited directly by using an electric arc igniter. The burning test also employed a recording of the combustion phenomenon using a digital high-speed camera. The result showed that the CL-NC, LC-NC, and CP-NC combustion underwent deflagration rather than detonation. The flame characteristics of CL-NC, LC-NC, and CP-NC can be observed and recorded in the high-speed imaging shown in Fig. 13. The images suggest that the burning of each NC resulted in a yellowish flame, a common characteristic of NC.³⁴ Linear deflagration was conducted to measure the CL-NC, LC-NC, and CP-NC burning rates. The still of the burning rate testing is shown in Fig. 14. CL-NC demonstrated the fastest burning duration and sequential burning rate, followed by LC-NC and CP-NC, as presented in Table 3. These differences in burning rate and duration could result from various factors, such as the physical form of nitrocellulose or access to oxidant (e.g.: compacted or uncompacted state, free fibers).⁶⁵ However, the burning test further confirms the NC in this work has a comparable burning rate with the referenced NC material.³⁵

Table 2 Summary of the relationship between the nitrogen content and cellulosic characteristics

	CL	LCC	CPC
Nitrogen content (%) (after nitration)	13.49	13.67	8.05
Cellulose microfibril morphology	Long, tubular twisted ribbon	Short, thin-walled tubular ribbon-like microfibril	Flat and dense surface appearance, with embedded spiral-shaped fibrils
Cellulose crystallinity (%)	75.52	75.09	59.63
Cellulose specific surface area ($\text{m}^2 \text{ g}^{-1}$)	0.51	0.70	0.59
Pre-nitration d_{hkl} (101) (\AA)	5.87	6.03	5.64
Post-nitration d_{hkl} (101) (\AA)	6.99	7.12	5.65

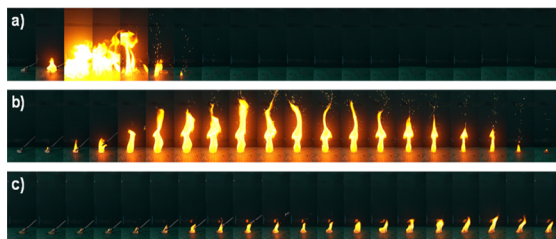


Fig. 13 Still of the deflagration sequences: (a) CL-NC, (b) LC-NC, and (c) CP-NC.

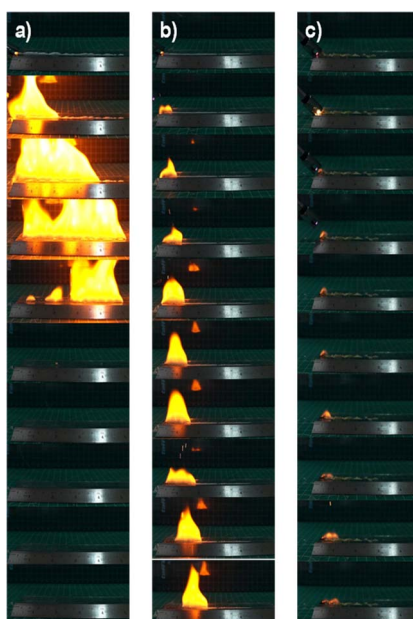


Fig. 14 Still of the linear deflagration testing: (a) CL-NC, (b) LC-NC, and (c) CP-NC.

Table 3 Burning duration and burning rate of CL-NC, LC-NC, and CP-NC

NC	Burning duration (s)	Burning rate (cm s^{-1})
CL-NC	0.68	5.38 ± 3.32
LC-NC	2.013	4.76 ± 2.58
CP-NC	11.584	0.92 ± 0.46

Conclusions

The nitrogen content of nitrocelluloses that resulted in this study exhibited an extensive cellulosic characteristic and morphology of cellulose in terms of nitration effectiveness. Cellulose was isolated from *Luffa cylindrica* and coffee pulp waste, which was then nitrated using a mixture of nitric acid and sulfuric acid with a nitric acid : sulfuric acid ratio of 1 : 3; cellulose : nitric acid ratio of 1 : 45 and nitration duration of 60 minutes, conducted at room temperature. Cotton linter was used as a point of reference in this study. The result showed that each cellulose source has distinct characteristics. LCC has the most similar characteristics to CL, which has a short, thin-walled tubular ribbon-like microfibril with 75.09% crystallinity and a specific surface area of $0.70 \text{ m}^2 \text{ g}^{-1}$. The morphological characteristic of LC, having favorable accessibility for foreign chemicals, allows it to result in nitrocellulose with a nitrogen content as high as 13.67%, slightly higher than CL with a value of 13.49%, which is high enough for even military-grade application. The calculation of change of the interplanar dimension through XRD characterization also confirms the high nitrogen content in post-nitrated CL and LCC, which is indicated by the higher d_{hkl} . Morphology is the most dependable characteristic that affects nitration compared to crystallinity and surface area. It is based on the result of the nitration of CPC, which is supposedly harder to access by the nitration reagent as it has a flat and dense surface morphology, resulting in far lower nitrogen content than LCC and CL-based cellulose, despite its higher crystallinity and specific surface area. Through this result, NC with high nitrogen content could be achieved by selecting the appropriate cellulose morphology and revealing its significance in enhancing the high nitrogen content of NC. In addition, the selective morphology allows NC to be prepared with high nitrogen content using technical grade nitration reagents, diminishing the use of harmful chemicals, such as fuming nitric acid. Thus, this work could contribute to supporting sustainable chemical processes.

Data availability

The bar diagrams depicting the nitrogen content of post-nitrated cotton linter, *Luffa cylindrica*, and coffee pulp celluloses; the diffraction angles and d_{hkl} of pre- and post-nitrated celluloses and higher-resolution scanning electron microscopy



images of cotton linter, *Luffa cylindrica*, and coffee pulp celluloses discussed in this article have been included as part of the ESI.†

Author contributions

Y. M., R. R. R., A. H.: conceptualization; R. R. R., Y. M.: methodology, formal analysis; R. R. R.: investigation, resources, visualization, writing – original draft; Y. M.: supervision; R. R. R., Y. M., A. H., T. D.: writing – review & editing; All authors read and approved the final manuscript.

Conflicts of interest

The authors report there are no conflicts to declare.

Acknowledgements

The authors would like to express their appreciation to the Indonesia Endowment Fund for Education Agency (LPDP) for supporting this research.

References

- 1 J. H. Bauer and T. P. Hughes, The preparation of the graded collodion membranes of Elford and their use in the study of filterable viruses, *J. Gen. Physiol.*, 1934, **18**, 143–162.
- 2 Z. Qin, Z. Huang, P. Pan, Y. Pan, R. Zuo, Y. Sun and X. Liu, A Nitrocellulose Paper-Based Multi-Well Plate for Point-of-Care ELISA, *Micromachines*, 2022, **13**, 1–11.
- 3 A. Meincke, D. Hausdorf, N. Gadsden, M. Baumeister, I. Derrick, R. Newman and A. Rizzo, Cellulose Nitrate Coatings on Furniture of the Company of Master Craftsmen, *J. Am. Inst. Conserv.*, 2009, **48**, 1–24.
- 4 J. Liu, *Nitrate Esters Chemistry and Technology*, Springer Nature Singapore, Singapore, 2019.
- 5 T. Urbanski, *Chemistry and Technology of Explosives*, Panstwowe Wydawnictwo Naukowe, Warsaw, 1st edn, 1965, vol. 2.
- 6 E. Morris, C. R. Pulham and C. A. Morrison, Structure and properties of nitrocellulose: approaching 200 years of research, *RSC Adv.*, 2023, **13**, 32321–32333.
- 7 J. L. Wertz, O. Bégué and J. P. Mercier, *Cellulose Science and Technology*, l'Ecole Polytechnique Fédérale de Lausanne Press, Lausanne, 2010.
- 8 M. I. Eremets, I. A. Trojan, A. G. Gavriliuk and S. A. Medvedev, Synthesis of High-Nitrogen Energetic Material, in *Static Compression of Energetic Materials*, ed. S. M. Peiris and G. J. Piermarini, Springer Berlin Heidelberg, Berlin, Heidelberg, 2008, pp. 75–97.
- 9 D. Kumar and A. J. Elias, The Explosive Chemistry of Nitrogen: A Fascinating Journey From 9th Century to the Present, *Resonance*, 2019, **24**, 1253–1271.
- 10 A. F. Tarchoun, D. Trache, T. M. Klapötke, S. Chelouche, M. Derradji, W. Bessa and A. Mezroua, A Promising Energetic Polymer from *Posidonia oceanica* Brown Algae: Synthesis, Characterization, and Kinetic Modeling, *Macromol. Chem. Phys.*, 2019, **220**, 1–15.
- 11 K. N. Onwukamike, S. Grelier, E. Grau, H. Cramail and M. A. R. Meier, Critical Review on Sustainable Homogeneous Cellulose Modification: Why Renewability Is Not Enough, *ACS Sustain. Chem. Eng.*, 2019, **7**, 1826–1840.
- 12 P. J. Wakelyn, N. R. Bertoniere, A. D. French, D. P. Thibodeaux, B. A. Triplett, M.-A. Rousselle, W. R. Goynes Jr, J. V. Edwards, L. Hunter, D. D. McAlister and G. R. Gamble, *Cotton Fiber Chemistry and Technology*, CRC Press, Taylor & Francis Group, Boca Raton, 2007.
- 13 L. Shen, E. Worrell and M. K. Patel, Environmental impact assessment of man-made cellulose fibres, *Resour. Conserv. Recycl.*, 2010, **55**, 260–274.
- 14 R. F. Miranda, Pembuatan Nitroselulosa dari Selulos- α Pelepah Sawit dengan Variasi Waktu Nitras dan Rasio Bahan Baku Terhadap Asam Penitras, *Pros. Semin. Nas. Tek. Kim. Teknol. Oleo dan Petrokimia Indones. (SNTK TOPI)*, 2013, 240–250.
- 15 Y. A. Gismatulina, V. V. Budaeva and G. V. Sakovich, Nitrocellulose Synthesis from Miscanthus Cellulose, *Propellants, Explos., Pyrotech.*, 2018, **43**, 96–100.
- 16 A. W. Handono and B. Kusmartono, Pembuatan Nitroselulosa Dari Kulit Kacang Tanah (Arachis hypogaea L.), *J. Inov. Proses*, 2017, **2**, 8–13.
- 17 Setiadi, Y. Mulyadi and B. Kusmartono, Optimasi Pembuatan Nitroselulosa dari Daun Nanas dengan Proses Delignifikasi Dalam Upaya Mewujudkan Sumber Energi Bersih dan Terbarukan, *Pros. Semin. Nas. XII Rekayasa Teknol. Ind. dan Inf. 2017 Sekol. Tinggi Teknol. Nas. Yogyakarta*, 2017, 304–309.
- 18 D. Trache, K. Khimeche, A. Mezroua and M. Benziane, Physicochemical properties of microcrystalline nitrocellulose from Alfa grass fibres and its thermal stability, *J. Therm. Anal. Calorim.*, 2016, **124**, 1485–1496.
- 19 F. T. Seta, S. Sugesti and R. Biantoro, Karakterisasi Nitroselulosa dari Pulp Larut Bambu Beema dan Bambu Industri, *J. Selulosa*, 2019, **9**, 25–32.
- 20 M. S. G. Jesuet, N. M. Musa, N. M. Idris, D. N. S. Musa and S. M. Bakansing, Properties of Nitrocellulose from Acacia mangium, *J. Phys.: Conf. Ser.*, 2019, **1358**, DOI: [10.1088/1742-6596/1358/1/012035](https://doi.org/10.1088/1742-6596/1358/1/012035).
- 21 M. F. Farhanudin and B. Kusmartono, Pembuatan Nitroselulosa Dari Tanaman Lidah Mertua (Sansevieria), *J. Inov. Proses.*, 2020, **5**, 1.
- 22 F. T. Seta, S. Sugesti and T. Kardiansyah, Pembuatan Nitroselulosa Dari Berbagai Pulp Larut Komersial Sebagai Bahan Baku Propelan, *J. Selulosa*, 2014, **4**, 97–106.
- 23 A. Kusmayati, S. Hudiyono, E. Saepudin and W. Basuki, The Effect of Ball Milling on The Nitrogen Content of Ramie (*Boehmeria nivea*) Nitrocellulose as Propellant Material, *Asian J. Res. Chem.*, 2011, **4**, 1881–1886.
- 24 Purnawan, Optimasi Proses Nitras pada Pembuatan Nitro Selulosa dari Serat Limbah Industri Sagu, *J. Rek. Pros.*, 2010, **4**, 30–34.



25 J. Credou, T. Berthelot, J. Credou and T. Berthelot, Cellulose: from biocompatible to bioactive material, *J. Mater. Chem. B*, 2014, **2**, 4767–4788.

26 T. Heinze, O. A. El Seoud and A. Koschella, *Cellulose Derivatives: Synthesis, Structure, and Properties*, Springer International Publishing, Cham, 2018.

27 V. Gehmeyr and H. Sixta, Pulp properties and their influence on enzymatic degradability, *Biomacromolecules*, 2012, **13**, 645–651.

28 L. C. E. Onelli and G. Patrignani, Spatial arrangement of the fibres in developing and mature endocarp of *Luffa cylindrica* Roem, *Plant Biosyst.*, 2001, **135**, 39–44.

29 M. Alhijazi, B. Safaei, Q. Zeeshan, M. Asmael, A. Eyyazian and Z. Qin, Recent developments in *Luffa* natural fiber composites: review, *Sustainability*, 2020, **12**, 1–25.

30 Y. Chen, N. Su, K. Zhang, S. Zhu, L. Zhao, F. Fang, L. Ren and Y. Guo, In-depth analysis of the structure and properties of two varieties of natural luffa sponge fibers, *Materials*, 2017, **10**, 479.

31 L. Ghali, S. Msahli, M. Zidi and F. Sakli, Effect of pre-treatment of *Luffa* fibres on the structural properties, *Mater. Lett.*, 2009, **63**, 61–63.

32 R. R. Rizkiansyah, Y. Mardiyati, A. Hariyanto and T. Dirgantara, Arabica Coffee Pulp Cellulose: Isolation, Morphology, and its Capabilities to be Modified into Cellulose Nitrate, *BIO Web Conf.*, 2023, **77**, DOI: [10.1051/bioconf/20237701001](https://doi.org/10.1051/bioconf/20237701001).

33 R. Datta, Acidogenic fermentation of lignocellulose-acid yield and conversion of components, *Biotechnol. Bioeng.*, 1981, **23**, 2167–2170.

34 J. Liu and M. Chen, A simplified method to predict the heat release rate of industrial nitrocellulose materials, *Appl. Sci.*, 2018, **8**, 1–14.

35 X. Zhang and B. L. Weeks, Preparation of sub-micron nitrocellulose particles for improved combustion behavior, *J. Hazard. Mater.*, 2014, **268**, 224–228.

36 J. C. O. Macuja, L. N. Ruedas and R. C. N. España, Utilization of Cellulose from *Luffa cylindrica* Fiber as Binder in Acetaminophen Tablets, *Advances in Environmental Chemistry*, 2015, **2015**, 1–8.

37 H. Abdellaoui, M. Raji, H. Essabir, R. Bouhfid and A. el Kacem Qaiss, in *Fibre-Reinforced Composites and Hybrid Composites*, ed. M. Jawaaid, M. Thariq and N. Saba, Woodhead Publishing, Duxford, 2019, vol. 6, pp. 103–122.

38 Y. Wu, J. Wu, F. Yang, C. Tang and Q. Huang, Effect of H₂O₂ bleaching treatment on the properties of finished transparent wood, *Polymers*, 2019, **11**, 1–13.

39 I. Bernal-Lugo, C. Jacinto-Hernandez, M. Gimeno, C. C. Montiel, F. Rivero-Cruz and O. Velasco, Highly efficient single-step pretreatment to remove lignin and hemicellulose from softwood, *BioResources*, 2019, **14**, 3567–3577.

40 W. Klunklin, S. Hinmo, P. Thipchai and P. Rachtanapun, Effect of Bleaching Processes on Physicochemical and Functional Properties of Cellulose and Carboxymethyl Cellulose from Young and Mature Coconut Coir, *Polymers*, 2023, **15**, 3376.

41 S. Susi, M. Ainuri, W. Wagiman and M. A. F. Falah, High-Yield Alpha-Cellulose from Oil Palm Empty Fruit Bunches by Optimizing Thermochemical Delignification Processes for Use as Microcrystalline Cellulose, *Int. J. Biomater.*, 2023, **2023**, DOI: [10.1155/2023/9169431](https://doi.org/10.1155/2023/9169431).

42 J. P. S. Morais, M. D. F. Rosa, M. De Souza Filho, L. D. Nascimento, D. M. Do Nascimento and A. R. Cassales, Extraction and characterization of nanocellulose structures from raw cotton linter, *Carbohydr. Polym.*, 2013, **91**, 229–235.

43 A. Sczostak, Cotton linters: an alternative cellulosic raw material, *Macromol. Symp.*, 2009, **280**, 45–53.

44 J. Gong, J. Li, J. Xu, Z. Xiang and L. Mo, Research on cellulose nanocrystals produced from cellulose sources with various polymorphs, *RSC Adv.*, 2017, **7**, 33486–33493.

45 M. K. D. Rambo and M. M. C. Ferreira, Determination of cellulose crystallinity of banana residues using near infrared spectroscopy and multivariate analysis, *J. Braz. Chem. Soc.*, 2015, **26**, 1491–1499.

46 S. Park, J. O. Baker, M. E. Himmel, P. A. Parilla and D. K. Johnson, Cellulose crystallinity index: measurement techniques and their impact on interpreting cellulase performance, *Biotechnol. Biofuels*, 2010, **3**, 10.

47 R. Hadiwibowo, E. Yuanita, E. Kustiyah and M. Chalid, Study of Crystallinity Index and Thermal Properties of Sweet Sorghum Fiber after Pressurized-Cooker Treatment, *Macromol. Symp.*, 2020, **391**, DOI: [10.1002/masy.201900129](https://doi.org/10.1002/masy.201900129).

48 S. N. Nikolsky, D. V. Zlenko, V. P. Melnikov and S. V. Stovbun, The fibrils untwisting limits the rate of cellulose nitration process, *Carbohydr. Polym.*, 2018, **204**, 232–237.

49 V. Chunilall, T. Bush and P. Tomas, in *Cellulose – Fundamental Aspects*, ed. T. van de Ven and L. Godbout, InTech, Rijeka, 2013, vol. 3, pp. 69–90.

50 A. James, M. R. Rahman, K. A. M. Said, D. Kanakaraju, A. Z. Sueraya, K. K. Kuok, M. K. B. Bakri and M. M. Rahman, A review of nanocellulose modification and compatibility barrier for various applications, *J. Thermoplast. Compos. Mater.*, 2023, **37**, DOI: [10.1177/08927057231205451](https://doi.org/10.1177/08927057231205451).

51 S. Liyanage, S. Acharya, P. Parajuli, J. L. Shamshina and N. Abidi, Production and surface modification of cellulose bioproducts, *Polymers*, 2021, **13**, 3433.

52 V. N. Krishnamurthy and T. L. Varghese, *The Chemistry and Technology of Solid Rocket Propellants (A Treatise on Solid Propellants)*, Allied Publishers Pvt. Ltd., New Delhi, 2017.

53 A. K. Yetisen, M. S. Akram and C. R. Lowe, Paper-based microfluidic point-of-care diagnostic devices, *Lab Chip*, 2013, **13**, 2210–2251.

54 I. M. Adekunle, Production of cellulose nitrate polymer from sawdust, *J. Chem.*, 2010, **7**, 709–716.

55 W. B. Robertson, Master theses, *Factor Governing the Nitration of Cellulose*, Cornell University, 1946.

56 D. P. Sun, B. Ma, C. L. Zhu, C. S. Liu and J. Z. Yang, Novel nitrocellulose made from bacterial cellulose, *J. Energ. Mater.*, 2010, **28**, 85–97.



57 X. Cao, F. Nan, J. Zhang, L. Chen, H. Gao and W. He, Effect of sulfuric residual acid on the physicochemical properties, thermal behavior, and decomposition kinetics of nitrocellulose, *Thermochim. Acta*, 2023, **729**, 179605.

58 J. Shi, D. Xing and J. Li, FTIR studies of the changes in wood chemistry from wood forming tissue under inclined treatment, *Energy Procedia*, 2012, **16**, 758–762.

59 J. Zhuang, M. Li, Y. Pu, A. J. Ragauskas and C. G. Yoo, Observation of potential contaminants in processed biomass using Fourier transform infrared spectroscopy, *Appl. Sci.*, 2020, **10**, 1–13.

60 S. H. Jamal, N. J. Roslan, N. A. A. Shah, S. A. M. Noor, K. K. Ong and W. M. Z. W. Yunus, Preparation and characterization of nitrocellulose from bacterial cellulose for propellant uses, *Mater. Today: Proc.*, 2019, **29**, 185–189.

61 A. Gainar, J. S. Stevens, C. Jaye, D. A. Fischer and S. L. M. Schroeder, NEXAFS Sensitivity to Bond Lengths in Complex Molecular Materials: A Study of Crystalline Saccharides, *J. Phys. Chem. B*, 2015, **119**, 14373–14381.

62 H. Ohsaki, K. Miura, A. Imai, M. Tada and M. A. Aegeerter, Structural analysis of SiO₂ gel films by high energy electron diffraction – code: CP3, *J. Sol-Gel Sci. Technol.*, 1994, **2**, 245–249.

63 M. Lee, *X-Ray Diffraction for Materials Research: from Fundamentals to Applications*, CRC Press, Boca Raton, 2016.

64 US Department of Defense, *Nitrocellulose (MIL-DTL-244C w/ amendment 1-20-May 2014)*, US Department of Defense, New Jersey, 2014.

65 R. Kuracina and Z. Szabov, Study into influence of different types of igniters on the explosion parameters of dispersed nitrocellulose powder, *J. Loss Prev. Process. Ind.*, 2022, **83**, DOI: [10.1016/j.jlp.2023.105017](https://doi.org/10.1016/j.jlp.2023.105017).

